Mass measurements of neutron-deficient Yb isotopes and nuclear structure at the extreme proton-rich side of the N=82 shell

Sönke Beck,[1,2,*] Brian Kootte,[3,4] Irene Dedes,[5,6] Timo Dickel,[1,2] Ania A. Kwiatkowski,[3,7] Eleni Marina Lykiardopoulou,[8,3] Wolfgang R. Plaß,[1,2] Moritz P. Reiter,[1,3,9] Corina Andreoiu,[10] Julian Bergmann,[1] Thomas Brunner,[11] Dominique Curien,[12] Jens Dilling,[3,8] Jerzy Dudek,[12,6] Eleanor Dunling,[3,13] Jake Flowerdew,[14] Abdelghafar Gaamouci,[15] Leigh Graham,[3] Gerald Gwinner,[4] Andrew Jacobs,[8,3] Renee Klawitter,[3] Yang Lan,[8] Erich Leistenschneider,[8,3] Nikolay Minkov,[16] Victor Monier,[3] Ish Mukul,[3] Stefan F. Paul,[3] Christoph Scheidenberger,[1,2,17] Robert I. Thompson,[14] James L. Tracy Jr.,[3] Michael Vansteenkiste,[3] Hua-Lei Wang,[18] Michael E. Wieser,[14] Christian Will,[1] and Jie Yang[6,18]

[1] *II. Physikalisches Institut, Justus-Liebig-Universität, 35392 Giessen, Germany*
[2] *GSI Helmholtzzentrum für Schwerionenforschung GmbH, 64291 Darmstadt, Germany*
[3] *TRIUMF, Vancouver, British Columbia V6T 2A3, Canada*
[4] *Department of Physics and Astronomy, University of Manitoba, Winnipeg, Manitoba R3T 2N2, Canada*
[5] *Institute of Nuclear Physics, Polish Academy of Sciences, PL-31 342 Kraków, Poland*
[6] *Institute of Physics, Marie Curie-Skłodowska University, PL-20 031 Lublin, Poland*
[7] *Department of Physics and Astronomy, University of Victoria, Victoria, British Columbia V8P 5C2, Canada*
[8] *Department of Physics and Astronomy, University of British Columbia, Vancouver, British Columbia V6T 1Z1, Canada*
[9] *School of Physics and Astronomy, University of Edinburgh, Edinburgh EH9 3FD, Scotland, United Kingdom*
[10] *Department of Chemistry, Simon Fraser University, Burnaby, British Columbia V5A 1S6, Canada*
[11] *Physics Department, McGill University, H3A 2T8 Montréal, Québec, Canada*
[12] *Université de Strasbourg, CNRS, IPHC UMR 7178, F-67 000 Strasbourg, France*
[13] *Department of Physics, University of York, York YO10 5DD, United Kingdom*
[14] *Department of Physics and Astronomy, University of Calgary, Calgary, Alberta T2N 1N4, Canada*
[15] *Faculté de Physique, University of Science and Technology Houari Boumediene, BP 32, El Alia, 16111 Bab Ezzouar, Algiers, Algeria*
[16] *Institute of Nuclear Research and Nuclear Energy, Bulgarian Academy of Sciences, BG-1784 Sofia, Bulgaria*
[17] *Helmholtz Forschungsakademie Hessen fr FAIR (HFHF), GSI Helmholtzzentrum fr Schwerionenforschung, Campus Gieen, 35392 Gieen, Germany*
[18] *School of Physics and Microelectronics, Zhengzhou University, Zhengzhou 450001, China*

(Dated: July 20, 2021)

High-accuracy mass measurements of neutron-deficient Yb isotopes have been performed at TRIUMF using TITAN's multiple-reflection time-of-flight mass spectrometer (MR-TOF-MS). For the first time, an MR-TOF-MS was used online simultaneously as isobar separator and as mass spectrometer, extending the measurements to two isotopes further away from stability than otherwise possible. The ground state masses of ^{150,153}Yb and the excitation energy of ^{151}Yb^m were measured for the first time. As a result, the persistence of the N=82 shell with almost unmodified shell gap energies is established up to the proton dripline. Furthermore, the puzzling systematics of the $h_{11/2}$-excited isomeric states of the N=81 isotones are unraveled using state-of-the-art mean field calculations.

Experimental and theoretical studies of exotic nuclei, *i.e.*, very short-lived nuclei far away from the valley of stability in the chart of the nuclides, present a unique and important way to gain general understanding of the atomic nucleus and the governing interactions of its constituents. Exotic nuclei reveal novel properties, unknown in more stable nuclei, such as nuclear halos and skins, and exotic decay modes [1, 2]. Deeper understanding of nuclear structure hinges on theoretical models. Extending experimental data towards the driplines is decisive for testing prediction capacities of theories, estimating the model uncertainties and thus for improving models and theories [3].

One striking effect, which may occur in exotic nuclei, is a change in the nuclear shell structure towards the proton or neutron driplines; shells can weaken or disappear, and new magic numbers appear [4, 5]. On the neutron-rich side of the nuclear chart, shell closures have been shown to vanish far from stability for the neutron numbers N=20 and N=28 [6, 7], and new shell closures have been found for N=32 and N=34 [8–15]. The N=82 shell closure has been studied for neutron-rich nuclei down to Cd [16–18]. The data in the neutron-deficient region are incomplete, and the evolution of the N=82 shell towards the proton dripline is not known. In this work, the N=82 shell closure is investigated by mass measurements up to the proton dripline.

Series of nuclear isomers are known to occur near shell closures. A unique sequence of isomers exists in the N=81 isotones with even Z, ranging from ^{131}Sn to ^{149}Er [19, 20]. This sequence is remarkable, because the excitation energies of these J^π=11/2$^-$ isomers stay approximately constant at 750 keV between ^{139}Ce and ^{149}Er [21–25], over a range of eleven isotones. Such an effect is

unique for isomers throughout the chart of the nuclides, and its origin has been considered enigmatic since its discovery more than 60 years ago [22, 25, 26]. The dependence of energy *vs.* total angular momentum within non-collective excitation regimes is usually strongly irregular according to nuclear mean-field theory [27]. Yet here, the experimental data of the series are extended, and the origin of the constant excitation energies is explained using state-of-the-art mean-field calculations.

A major challenge for experiments with exotic nuclei at radioactive ion beam facilities is isobaric contamination. Nuclei closer to stability and molecules are usually produced with rates many orders of magnitude higher than those of the nuclei of interest and hamper measurements of the exotic nuclei. Recently, multiple-reflection time-of-flight mass spectrometers (MR-TOF-MS) [28, 29] have been established as isobar separators [30, 31] and even isomer separators [32]. They feature very high mass separation powers of several 10^5 and short cycle times, enabling access to very short-lived ($\approx$ ms) nuclides and high ion rates (10^6 ions/s). MR-TOF-MS can also be used for direct mass measurements of exotic nuclei [12, 33–35] and diagnostics purposes [36–38]. In an MR-TOF-MS, ions are cooled in a radio-frequency (RF) ion trap (injection trap), injected into a time-of-flight (TOF) analyzer, in which the ions are stored between two ion reflectors and dispersed in TOF according to their mass-to-charge ratios. Mass separation is then achieved by the subsequent removal of the unwanted ions using a fast-switching deflector, such as a Bradbury-Nielsen gate [30], a pulsed drift tube [39], or one of the reflectors [40]. A novel method for mass separation in an MR-TOF-MS is the dynamical re-trapping of the ions in the injection trap after the TOF dispersion procedure [41]. This re-trapping technique is highly mass-selective; the ions of interest can be stored, while other ions are removed. In contrast to the other methods, it allows an MR-TOF-MS to act as an isobar separator for its own mass measurements. It has been developed for the MR-TOF-MS [42, 43] at TRIUMF's Ion Trap for Atomic and Nuclear Science (TITAN) [44], but it could also be used to add one or several stages of isobar separation to mass measurements in other MR-TOF-MS world-wide.

In this work, mass-selective re-trapping has been employed for the first time on-line. High-accuracy mass measurements of neutron-deficient Yb isotopes were performed using TITAN's MR-TOF-MS. The nuclei were produced in spallation reactions at the ISAC facility [45] by impinging a 480 MeV proton beam with a current of 25 to 45 μA from the TRIUMF cyclotron onto a Ta target. Yb atoms that left the target were ionized by the TRIUMF resonant ionization laser ion source TRILIS [46], using a two-step resonant laser excitation scheme into a high-lying Rydberg state [47, 48]. Ions were extracted and separated using ISAC's high-resolution mass separator [49] at a mass separation power of about 2000. The

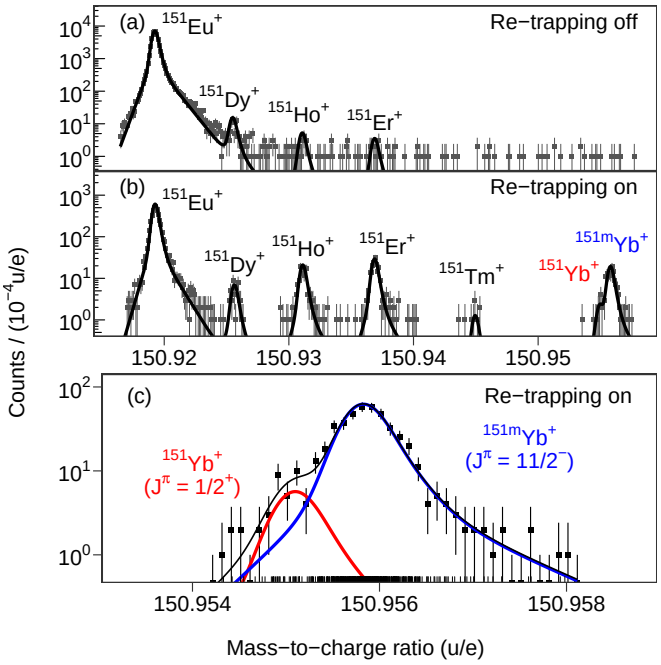

FIG. 1. Mass spectra at mass-to-charge ratio 151 u/e (a) without re-trapping, (b) with re-trapping set for ^{151}Yb, (c) zoom to the Yb region with re-trapping, showing the ^{151}Yb nuclear ground and isomeric state. The ions performed 335 IT in the analyzer, corresponding to a TOF of 8.14 ms. The curves represent hyper-EMG [52] fits to the data. Note the different abundance scales. For both spectra (a) and (b) the measurement time was 760 s; for (b) the incoming rate was increased; (c) contains all data taken during about 3 h with different proton currents on the target.

isobaric beam, consisting mostly of singly-charged Eu, Dy, Ho, Er, Tm, Yb, BaF and CeO ions, was transported to the TITAN facility, cooled and bunched in the TITAN RF quadrupole (RFQ) cooler buncher [50] and injected into the MR-TOF-MS. There, the ions were transported to the injection trap, cooled and injected into the TOF analyzer, where they performed one time-focus shift turn [51] and about 330 isochronous turns (IT), corresponding to a TOF of about 8 ms. Then the ions were ejected onto a detector. A mass-resolving power of about 270,000 (FWHM) was achieved. For measurements, in which the isobaric contamination was too high to observe Yb ions, the MR-TOF-MS was first used as an isobar separator: after TOF dispersion of the ions in the analyzer, the ions of interest were re-trapped in the injection trap. Then, they were re-cooled and injected again into the analyzer for the subsequent mass measurement procedure. The overall cycle time was 20 ms. After each mass measurement, a spectrum was taken without resonant laser ionization to verify the identification of the Yb ions.

Figure 1 shows mass spectra measured without and with re-trapping. The mass separation power amounts to 35,000. To avoid deterioration of the mass measurement accuracy due to ion-ion interactions, the beam was

Nuclide	Calibrant	ME_{TITAN} (keV/c^2)	ME_{AME20} (keV/c^2)	ΔME (keV/c^2)
^{157}Yb	$^{157}Tm^+$	−53395(54)	−53420(11)	25(55)
^{156}Yb	$^{156}Tm^+$	−53331(55)	−53266(9)	−65(56)
^{155}Yb	$^{155}Eu^+$	−50514(45)	−50503(17)	−11(48)
^{154}Yb	$^{138}Ce^{16}O^+$	−49934(45)	−49932(17)	−2(48)
^{153}Yb	$^{153}Dy^+$	−47102(46)	—	—
^{152}Yb	$^{136}Ce^{16}O^+$	−46061(46)	−46270(150)	209(157)
^{151}Yb	$^{151}Er^+$	−41297(114)	−41540(300)	243(321)
^{151}Yb^m	$^{151}Er^+$	−40617(49)	—	—
^{150}Yb	$^{150}Dy^+$	−38635(44)	—	—

TABLE I. List of measured mass excess values of Yb isotopes, ME_{TITAN}. Mass excess values from the AME2020, ME_{AME20}, and the deviation $\Delta ME = ME_{TITAN} - ME_{AME20}$ [54], are given for comparison, where available.

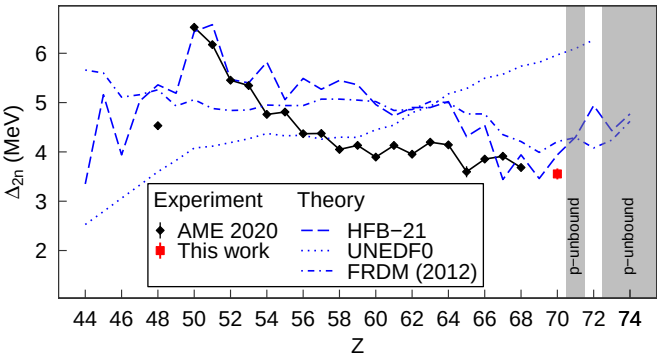

FIG. 2. Evolution of the two-neutron-shell gap Δ_{2n} at N=82 as a function of the proton number Z and predictions of the theoretical models HFB21 [57], UNEDF0 [58], and FRDM2012 [59]. Experimental data are from the AME2020 [54] and this work. Regions of proton-unbound nuclides are indicated [54, 60]. Most error bars are hidden in the symbols, lines are drawn to guide the eye.

attenuated in the ISAC beam line to about one ion per species per cycle detected in the MR-TOF-MS. Using mass-selective re-trapping, the rate of contaminant ions was reduced by at least three orders of magnitude, and the rate of incoming ions could therefore be increased by a corresponding factor by increasing the proton current on the target and by reducing the attenuation. As shown in Fig. 1, the nuclides ^{151}Tm and ^{151}Yb could only be measured with re-trapping. Similarily, the measurement of ^{150}Yb required re-trapping. The re-trapping increases the dynamic range of the measurement to five orders of magnitude, a value which is rarely achieved in mass spectrometry. It also reduces the total number of ions that reach the detector; this minimizes the background resulting from radioactivity implanted on the detector.

For the analysis of the data, the recorded TOF data were converted to mass data using an isobaric ion species present in the mass spectrum to provide a time-resolved calibration [53]. The mass spectra were analyzed by fitting hyper-EMG functions [52] to the unbinned mass data using weighted maximum likelihood estimation [53]. The isotopes of interest and their respective calibrants are listed in Table I. The mass values of the calibrants were taken from the Atomic Mass Evaluation AME2020 [54]. The dominating contribution to the systematic uncertainty are shifts in the TOF due to voltage ringing caused by the switching of the reflector voltages [55, 56]. Its relative value amounts to 3×10^{-7}.

The ground state masses of eight Yb isotopes were measured (Table I). For $^{154-157}$Yb, the masses were already well known, and the present results are in good agreement with the AME2020 [54]. The masses of ^{151}Yb and ^{152}Yb were measured directly for the first time, and their uncertainties could be reduced by a factor of three. The masses of ^{150}Yb and ^{153}Yb were measured for the first time.

With these results, the N=82 shell closure can be examined in the extreme proton-rich region. Figure 2 shows the empirical two-neutron-shell gap $\Delta_{2n}(Z,N) = S_{2n}(Z,N) - S_{2n}(Z,N+2)$, where $S_{2n}(Z,N) = B(Z,N) - B(Z,N-2)$ is the two-neutron separation energy and $B(Z,N)$ is the binding energy, for different N=82 isotones. The two-neutron-shell gap shows pronounced maxima when crossing closed shells. From the proton shell closure at Z=50, the two-neutron-shell gap decreases, though from Z=58 onward, the reduction is only weak. So far, the most proton-rich nuclide, for which Δ_{2n} was known, was ^{150}Er (Z=68). The newly determined value for ^{152}Yb (Z=70), despite being the lowest value found so far, clearly establishes that the shell persists with almost unmodified shell gap energy up to the proton dripline. The dripline is expected to lie between ^{152}Yb and ^{153}Lu (Z=71) [54, 60]. The experimental data are compared with different theoretical models, the macroscopic-microscopic finite-range droplet model FRDM(2012) [59], and two microscopic models, the Hartree-Fock-Bogoliubov model with BSk21 Skyrme interaction (HFB-21) [57], and the energy density functional UNEDF0 [58]. Although HFB-21 comes closest to the measured values, in particular for the most proton-rich isotones, none of these models fully reproduces the experimental trend. This fact highlights the importance of measurements for model improvements and model error estimates.

Furthermore, the mass of ^{153}Yb provides an anchor point for the α decay chains from ^{173}Hg to ^{153}Yb and from ^{170}Au to ^{154}Lu and thus determines the absolute masses of nine more nuclides and fix the mass surface in this region of the chart of nuclides [61, 62].

A $J^\pi = 11/2^-$ isomer has been observed in ^{151}Yb previously [63–65], but in this work its excitation energy was measured for the first time (Fig. 1c). In total, 460 events were detected with an isomer-to-ground state ratio of 11.1(3.1), corresponding to 38 events in the ground state. The measured excitation energy is 679(105) keV;

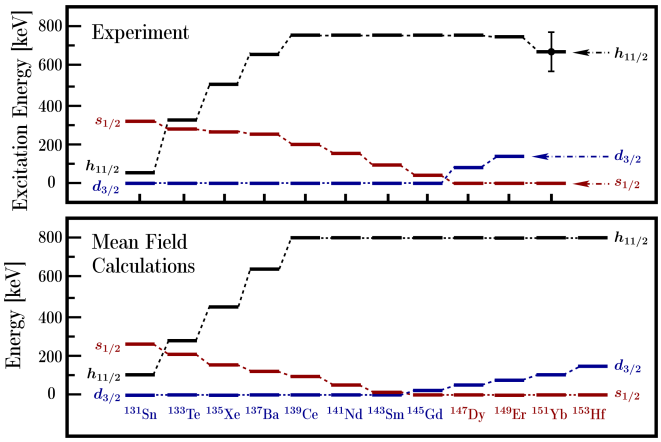

FIG. 3. (a) Top panel: Measured excitation energies of isomers in the even-Z N=81 isotones from Sn to Yb [19, 25]. The value for ^{151}Yb results from the present work. Most error bars are invisible within the scale of the figure. Note the constancy of the $h_{11/2}$ excitation energy from Ce to Yb. (b) Bottom panel: Corresponding results obtained using mean-field calculations with universal parametrization of the Woods-Saxon Hamiltonian. From Nd (Z=60) to Hf (Z=72), the filled proton levels are near-degenerate, *cf.* Fig. 4.

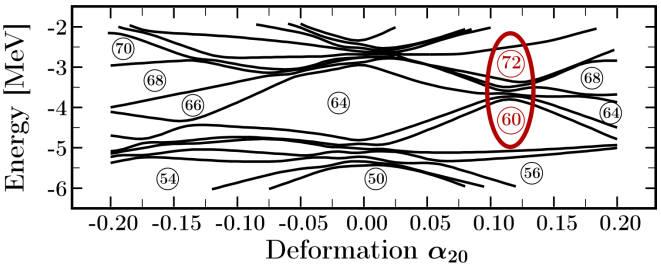

FIG. 4. Single proton energies as functions of the quadrupole deformation α_{20}, calculated using the Woods-Saxon Hamiltonian. The numbers in the circles represent the numbers of protons that can fill the levels below the circles. Note a near-degeneracy of 6 levels at small prolate deformations, indicated with oval curve, *cf.* Nd–Hf evolution in Fig. 3

it falls in line with the excitation energy of about 750 keV of J^π=11/2$^-$ isomers in the even-Z, N=81 isotones from ^{139}Ce onward. The experimental data are shown in Fig. 3a. The systematic trend suggests the assignment of the measured Yb isomer as J^π=11/2$^-$[25, 64]. The J^π=1/2$^+$, 3/2$^+$, and 11/2$^-$ states are neutron-hole states below the closed shell and can be associated with the $s_{1/2}$, $d_{3/2}$, $h_{11/2}$ orbitals, respectively. The fact that the excitation energies are constant has not been explained so far [22, 25, 26].

In order to resolve this long-standing riddle, mean-field calculations were performed. The phenomenological, deformed Woods-Saxon Hamiltonian in its so-called universal parametrization, for which its parameters are fixed throughout the chart of nuclides, was employed [66–70]. Its use is supported by the fact that it has been successfully applied in numerous nuclear structure calculations. Furthermore, it has recently been tested extensively from the point of view of prediction uncertainties and elimination of parametric correlations [71], which are known to destroy – often completely – model prediction capacities [72].

Potential-energy calculations using the Strutinsky method [73] were performed for all even-Z isotones from Sn to Hf. Partial results are shown in Fig. 3b. The J^π=3/2$^+$ ground-states with even-Z from Sn to Gd can be associated with $d_{3/2}$, and J^π=1/2$^+$ with $s_{1/2}$ orbitals from Dy to Hf. The latter orbital does not couple with the spin-orbit field at all, whereas the former does so only very weakly, so that their crossing at Gd and Dy reflects mainly the evolution of the central potential with Z.

Calculations show the impact of the shell closures at Z=50 and N=82, in that the ground-state equilibrium shapes remain spherical for the Sn, Te, Xe and Ba isotones, though the potential stiffness decreases. They predict non-spherical (oblate) quadrupole equilibrium shapes for ^{139}Ce and heavier isotones, while predicting small but increasingly prolate shapes for the J^π=11/2$^-$ isomers. This evolution coincides with the evolution of the energies of the isomers, which increase from about 40 keV in ^{131}Sn to about 750 keV in ^{139}Ce, i.e., within the zone of spherical ground-states. Stabilization at about 750 keV, starting with Ce (Z=58), coincides with the mean-field predictions of the slightly prolate quadrupole shapes with quadrupole deformations of $\alpha_{20} \approx 0.10$ at the J^π=11/2$^-$ isomeric energy minima. The calculations also show that the trend of constant J^π=11/2$^-$ isomer excitation energies continues for ^{153}Hf.

Below spherical closed neutron shells (here N=82), K-isomers usually correspond to nucleonic configurations with maximum alignment of the angular-momentum j, *i.e.* with projection $m_j = j$, at slightly prolate quadrupole shapes [27]. Calculations suggest that $h_{11/2}$-isomers have typical prolate deformations of $\alpha_{20} \approx 0.1$. The underlying stabilizing structural element is the very high single-nucleonic (proton) density at $\alpha_{20} \approx 0.12$ (Fig. 4), where six proton levels lie very close together. According to the Strutinsky shell-correction approach, the corresponding shell-energies are strongly negative and nearly constant, stabilizing the corresponding shapes with isomer energies at about 800 keV.

In summary, high-accuracy mass measurements of neutron-deficient Yb isotopes have been performed. They were enabled by the first-ever simultaneous online use of an MR-TOF-MS as isobar separator and as mass spectrometer, employing mass-selective re-trapping, and thus extending the measurements to two isotopes further away from stability than otherwise possible. The persistence of the N=82 shell with almost unmodified shell gap energies was established up to the expected location of the proton dripline. Furthermore, the results extend the

knowledge of excitation energies of the unique $J^\pi=11/2^-$ isomers in even-Z, N=81 isotones. The structural properties of this sequence were analyzed, and the constant excitation energies over a range of 13 isotones was explained. Application of the mass-selective re-trapping is not limited to TITAN, but could also be employed with other MR-TOF-MS world-wide to extend the reach of mass measurements with these devices by two or more isotopes towards exoticity. Since its first use in this experiment, this technique is now regularly applied in TITAN's MR-TOF-MS.

We would like to thank J. Lassen and the TRILIS ion source group for the excellent beam conditions. This work was supported by the German Research Foundation (DFG), grant No. SCHE 1969/2-1, by the German Federal Ministry for Education and Research (BMBF), grant No. 05P16RGFN1 and 05P19RGFN1, by the Hessian Ministry for Science and Art through the LOEWE Center HICforFAIR, by the JLU and GSI under the JLU-GSI strategic Helmholtz partnership agreement, by the Polish National Science Centre under Contract No. 2016/21/B/ST2/01227, by the Natural Sciences and Engineering Research Council of Canada (NSERC) under grants SAPIN-2018-00027 and RGPAS-2018-522453 and by the UKRI Science and Technology Facilities Council (STFC) grant No. ST/P004008/1. Support from the National Natural Science Foundation of China, grant No. 11975209, and the Physics Research and Development Program of Zhengzhou University, grant No. 32410017 are acknowledged. TRIUMF receives federal funding via NRC-CNRC. N.M. acknowledges the support by the FAIR Phase-0 project and by Bulgarian NSF contract KP-06-N48/1. E.D. acknowledges the support by the Canada-UK Foundation.

* Corresponding author: s.beck@gsi.de

[1] K. Riisager, Rev. Mod. Phys. **66**, 1105 (1994).
[2] M. Pfützner, M. Karny, L. V. Grigorenko, and K. Riisager, Rev. Mod. Phys. **84**, 567 (2012).
[3] I. Dedes and J. Dudek, Phys. Rev. C **99**, 054310 (2019).
[4] O. Sorlin and M.-G. Porquet, Prog. Part. Nucl. Phys. **61**, 602 (2008).
[5] R. Kanungo, Phys. Scripta **T152**, 014002 (2013).
[6] C. Thibault, R. Klapisch, C. Rigaud, A. M. Poskanzer, R. Prieels, L. Lessard, and W. Reisdorf, Phys. Rev. C **12**, 644 (1975).
[7] F. Sarazin, H. Savajols, W. Mittig, F. Nowacki, N. A. Orr, Z. Ren, P. Roussel-Chomaz, G. Auger, D. Baiborodin, A. V. Belozyorov, *et al.*, Phys. Rev. Lett. **84**, 5062 (2000).
[8] A. T. Gallant, J. C. Bale, T. Brunner, U. Chowdhury, S. Ettenauer, A. Lennarz, D. Robertson, V. V. Simon, A. Chaudhuri, J. D. Holt, *et al.*, Phys. Rev. Lett. **109**, 032506 (2012).
[9] F. Wienholtz, D. Beck, K. Blaum, C. Borgmann, M. Breitenfeldt, R. B. Cakirli, S. George, F. Herfurth, J. D. Holt, M. Kowalska, *et al.*, Nature **498**, 346 (2013).
[10] M. Rosenbusch, P. Ascher, D. Atanasov, C. Barbieri, D. Beck, K. Blaum, C. Borgmann, M. Breitenfeldt, R. B. Cakirli, A. Cipollone, *et al.*, Phys. Rev. Lett. **114**, 202501 (2015).
[11] X. Xu, M. Wang, Y.-H. Zhang, H.-S. Xu, P. Shuai, X.-L. Tu, Y. A. Litvinov, X.-H. Zhou, B.-H. Sun, Y.-J. Yuan, *et al.*, Chinese Physics C **39**, 104001 (2015).
[12] E. Leistenschneider, M. P. Reiter, S. Ayet San Andrés, B. Kootte, J. D. Holt, P. Navrátil, C. Babcock, C. Barbieri, B. R. Barquest, J. Bergmann, *et al.*, Phys. Rev. Lett. **120**, 062503 (2018).
[13] D. Steppenbeck, S. Takeuchi, N. Aoi, P. Doornenbal, M. Matsushita, H. Wang, H. Baba, N. Fukuda, S. Go, M. Honma, *et al.*, Nature **502**, 207 (2013).
[14] S. Michimasa, M. Kobayashi, Y. Kiyokawa, S. Ota, D. S. Ahn, H. Baba, G. P. A. Berg, M. Dozono, N. Fukuda, T. Furuno, *et al.*, Phys. Rev. Lett. **121**, 022506 (2018).
[15] E. Leistenschneider, E. Dunling, G. Bollen, B. A. Brown, J. Dilling, A. Hamaker, J. D. Holt, A. Jacobs, A. A. Kwiatkowski, T. Miyagi, *et al.* (The LEBIT Collaboration and the TITAN Collaboration), Phys. Rev. Lett. **126**, 042501 (2021).
[16] D. Atanasov, P. Ascher, K. Blaum, R. B. Cakirli, T. E. Cocolios, S. George, S. Goriely, F. Herfurth, H.-T. Janka, O. Just, *et al.*, Phys. Rev. Lett. **115**, 232501 (2015).
[17] R. Knöbel, M. Diwisch, F. Bosch, D. Boutin, L. Chen, C. Dimopoulou, A. Dolinskii, B. Franczak, B. Franzke, H. Geissel, *et al.*, Physics Letters B **754**, 288 (2016).
[18] V. Manea, J. Karthein, D. Atanasov, M. Bender, K. Blaum, T. E. Cocolios, S. Eliseev, A. Herlert, J. D. Holt, W. J. Huang, *et al.*, Phys. Rev. Lett. **124**, 092502 (2020).
[19] F. Kondev, M. Wang, W. Huang, S. Naimi, and G. Audi, Chin. Phys. C **45**, 030001 (2021).
[20] From ENSDF database as of October, 2020, https://www.nndc.bnl.gov/ensarchivals/.
[21] B. H. Ketelle, H. Thomas, and A. R. Brosi, Phys. Rev. **103**, 190 (1956).
[22] K. Kotajima and H. Morinaga, Nucl. Phys. **16**, 231 (1960).
[23] G. Jansen, H. Morinaga, and C. Signorini, Nucl. Phys. A **128**, 247 (1969).
[24] K. Toth, A. Rainis, C. Bingham, E. Newman, H. Carter, and W.-D. Schmidt-Ott, Phys. Lett. B **56**, 29 (1975).
[25] K. S. Toth, Y. A. Ellis-Akovali, F. T. Avignone, R. S. Moore, D. M. Moltz, J. M. Nitschke, P. A. Wilmarth, P. K. Lemmertz, D. C. Sousa, and A. L. Goodman, Phys. Rev. C **32**, 342 (1985).
[26] K. Heyde and P. J. Brussaard, Z. Phys. A **259**, 15 (1973).
[27] M. J. A. de Voigt, J. Dudek, and Z. Szymanski, Rev. Mod. Phys. **55**, 949 (1983).
[28] H. Wollnik and M. Przewloka, Int. J. Mass Spectrom. Ion Processes **96**, 267 (1990).
[29] W. R. Plaß, T. Dickel, and C. Scheidenberger, Int. J. Mass Spectrom. **349**, 134 (2013).
[30] W. R. Plaß, T. Dickel, U. Czok, H. Geissel, M. Petrick, K. Reinheimer, C. Scheidenberger, and M. I. Yavor, Nucl. Instrum. Methods B **266**, 4560 (2008).
[31] R. N. Wolf, D. Beck, K. Blaum, C. Böhm, C. Borgmann, M. Breitenfeldt, N. Chamel, S. Goriely, F. Herfurth, M. Kowalska, *et al.*, Phys. Rev. Lett. **110**, 041101 (2013).
[32] T. Dickel, W. R. Plaß, S. Ayet San Andrés, J. Ebert, H. Geissel, E. Haettner, C. Hornung, I. Miskun, S. Pietri,

S. Purushothaman, *et al.*, Phys. Lett. B **744**, 137 (2015).
[33] F. Wienholtz, D. Beck, K. Blaum, C. Borgmann, M. Breitenfeldt, R. B. Cakirli, S. George, F. Herfurth, J. D. Holt, M. Kowalska, *et al.*, Nature **498**, 346 (2013).
[34] Y. Ito, P. Schury, M. Wada, F. Arai, H. Haba, Y. Hirayama, S. Ishizawa, D. Kaji, S. Kimura, H. Koura, *et al.*, Phys. Rev. Lett. **120**, 152501 (2018).
[35] C. Hornung, D. Amanbayev, I. Dedes, G. Kripko-Koncz, I. Miskun, N. Shimizu, S. Ayet San Andrés, J. Bergmann, T. Dickel, J. Dudek, *et al.*, Phys. Lett. B **802**, 135200 (2020).
[36] S. Purushothaman, M. P. Reiter, E. Haettner, P. Dendooven, T. Dickel, H. Geissel, J. Ebert, C. Jesch, W. R. Plaß, M. Ranjan, *et al.*, Eur. Phys. Lett. **104**, 42001 (2013).
[37] R. Wolf, F. Wienholtz, D. Atanasov, D. Beck, K. Blaum, C. Borgmann, F. Herfurth, M. Kowalska, S. Kreim, Y. A. Litvinov, *et al.*, Int. J. Mass Spectrom. **349-350**, 123 (2013).
[38] M. P. Reiter, F. Ames, C. Andreoiu, S. Ayet San Andrés, C. Babcock, B. R. Barquest, J. Bergmann, J. Bollig, T. Brunner, T. Dickel, *et al.*, Nucl. Instrum. Methods B **463**, 431 (2020).
[39] F. Wienholtz, S. Kreim, M. Rosenbusch, L. Schweikhard, and R. Wolf, Int. J. Mass Spectrom. **421**, 285 (2017).
[40] J. T. Johnson, I. J. Carrick, G. S. Eakins, and S. A. McLuckey, Anal. Chem. **91**, 8789 (2019).
[41] T. Dickel, W. R. Plaß, W. Lippert, J. Lang, M. I. Yavor, H. Geissel, and C. Scheidenberger, J. Am. Soc. Mass Spectrom. **28**, 1079 (2017).
[42] C. Jesch, T. Dickel, W. R. Plaß, D. Short, S. Ayet San Andres, J. Dilling, H. Geissel, F. Greiner, J. Lang, K. G. Leach, *et al.*, Hyperfine Interact. **235**, 97 (2015).
[43] T. Dickel, S. Ayet San Andres, S. Beck, J. Bergmann, J. Dilling, F. Greiner, C. Hornung, A. Jacobs, G. Kripko-Koncz, A. Kwiatkowski, *et al.*, Hyperfine Interact. **240** (2019).
[44] J. Dilling, R. Baartman, P. Bricault, M. Brodeur, L. Blomeley, F. Buchinger, J. Crawford, J. R. C. Lopez-Urrutia, P. Delheij, M. Froese, *et al.*, Int. J. Mass Spectrom. **251**, 198 (2006).
[45] M. Dombsky, D. Bishop, P. Bricault, D. Dale, A. Hurst, K. Jayamanna, R. Keitel, M. Olivo, P. Schmor, and G. Stanford, Rev. Sci. Instrum. **71**, 978 (2000).
[46] S. Raeder, H. Heggen, J. Lassen, F. Ames, D. Bishop, P. Bricault, P. Kunz, A. Mjøs, and A. Teigelhöfer, Rev. Sci. Instrum. **85**, 033309 (2014).
[47] J. Lassen, R. Li, S. Raeder, X. Zhao, T. Dekker, H. Heggen, P. Kunz, C. D. P. Levy, M. Mostanmand, A. Teigelhöfer, and F. Ames, Hyperfine Interact. **238**, 33 (2017).
[48] H. Backe, P. Kunz, W. Lauth, A. Dretzke, R. Horn, T. Kolb, M. Laatiaoui, M. Sewtz, D. Ackermann, M. Block, *et al.*, Eur. Phys. J. D **45**, 99 (2007).
[49] P. Bricault, R. Baartman, M. Dombsky, A. Hurst, C. Mark, G. Stanford, and P. Schmor, Nucl. Phys. A **701**, 49 (2002).
[50] T. Brunner, M. J. Smith, M. Brodeur, S. Ettenauer, A. T. Gallant, V. V. Simon, A. Chaudhuri, A. Lapierre, E. Mane, R. Ringle, *et al.*, Nucl. Instrum. Methods A **676**, 32 (2012).
[51] T. Dickel, M. I. Yavor, J. Lang, W. R. Plaß, W. Lippert, H. Geissel, and C. Scheidenberger, Int. J. Mass Spectrom. **412**, 1 (2017).
[52] S. Purushothaman, S. Ayet San Andrés, J. Bergmann, T. Dickel, J. Ebert, H. Geissel, C. Hornung, W. R. Plaß, C. Rappold, C. Scheidenberger, *et al.*, Int. J. Mass Spectrom. **421**, 245 (2017).
[53] S. Ayet San Andrés, C. Hornung, J. Ebert, W. R. Plaß, T. Dickel, H. Geissel, C. Scheidenberger, J. Bergmann, F. Greiner, E. Haettner, *et al.*, Phys. Rev. C **99**, 064313 (2019).
[54] M. Wang, W. Huang, F. Kondev, G. Audi, and S. Naimi, Chin. Phys. C **45**, 030003 (2021).
[55] C. Will, *TITAN's Multiple-Reflection Time-of-Flight Mass Spectrometer and Isobar Separator – Characterization and First Experiments*, Bachelor thesis, Justus Liebig University Gießen (2017).
[56] M. P. Reiter, S. Ayet San Andrés, E. Dunling, B. Kootte, E. Leistenschneider, C. Andreoiu, C. Babcock, B. R. Barquest, J. Bollig, T. Brunner, *et al.*, Phys. Rev. C **98**, 024310 (2018).
[57] S. Goriely, N. Chamel, and J. M. Pearson, Phys. Rev. C **82**, 035804 (2010).
[58] M. Kortelainen, T. Lesinski, J. Moré, W. Nazarewicz, J. Sarich, N. Schunck, M. V. Stoitsov, and S. Wild, Phys. Rev. C **82**, 024313 (2010).
[59] P. Möller, A. J. Sierk, T. Ichikawa, and H. Sagawa, At. Data Nucl. Data Tables **109**, 1 (2016).
[60] L. Neufcourt, Y. Cao, S. Giuliani, W. Nazarewicz, E. Olsen, and O. B. Tarasov, Phys. Rev. C **101**, 014319 (2020).
[61] M. Wang, G. Audi, F. G. Kondev, W. J. Huang, S. Naimi, and X. Xu, Chin. Phys. C **41** (2017).
[62] E. M. Lykiardopoulou *et al.*, (in preparation).
[63] P. Kleinheinz, B. Rubio, M. Ogawa, M. Piiparinen, A. Plochocki, D. Schardt, R. Barden, O. Klepper, R. Kirchner, and E. Roeckl, Z. Phys. A **323**, 705 (1985).
[64] K. Toth, Y. Ellis-Akovali, J. Nitschke, P. Wilmarth, P. Lemmertz, D. Moltz, and F. Avignone, Phys. Lett. B **178**, 150 (1986).
[65] Y. A. Akovali, K. S. Toth, A. L. Goodman, J. M. Nitschke, P. A. Wilmarth, D. M. Moltz, M. N. Rao, and D. C. Sousa, Phys. Rev. C **41**, 1126 (1990).
[66] J. Dudek and T. Werner, Journal of Physics G: Nuclear Physics **4**, 1543 (1978).
[67] J. Dudek, A. Majhofer, J. Skalski, T. Werner, S. Cwiok, and W. Nazarewicz, Journal of Physics G: Nuclear Physics **5**, 1359 (1979).
[68] J. Dudek, W. Nazarewicz, and T. Werner, Nuclear Physics A **341**, 253 (1980).
[69] J. Dudek, Z. Szymański, and T. Werner, Phys. Rev. C **23**, 920 (1981).
[70] S. Cwiok, J. Dudek, W. Nazarewicz, J. Skalski, and T. Werner, Computer Physics Communications **46**, 379 (1987).
[71] A. Gaamouci, I. Dedes, J. Dudek, A. Baran, N. Benhamouda, D. Curien, H. L. Wang, and J. Yang, Phys. Rev. C **103**, 054311 (2021).
[72] I. Dedes and J. Dudek, Physica Scripta **93**, 044003 (2018).
[73] V. Strutinsky, Nucl. Phys. A **95**, 420 (1967).